

# Partial loss compensation in dielectric-loaded plasmonic waveguides at near infra-red wavelengths

C. Garcia,<sup>1,2,\*</sup> V. Coello,<sup>3</sup> Z. Han,<sup>2</sup> I. P. Radko,<sup>2</sup> and S. I. Bozhevolnyi<sup>2</sup>

<sup>1</sup>Doctorado en Ingeniería Física Industrial, Facultad de Ciencias Físico Matemáticas, Universidad Autónoma de Nuevo León, Ave. Universidad s/n. Cd. Universitaria, San Nicolás de los Garza, N.L., C.P. 66450, Mexico

<sup>2</sup>Institute of Technology and Innovation (ITI) University of Southern Denmark, Niels Bohrs Allé 1, DK-5230 Odense M, Denmark

<sup>3</sup>Centro de Investigación Científica y Educación Superior de Ensenada, Unidad Monterrey, Km 9.5 Carretera Nueva al Aeropuerto. PIIT. Apodaca, N.L. C.P.66600, Mexico

\*cegarcia@cicese.mx

**Abstract:** We report on the fabrication and characterization of straight dielectric-loaded surface plasmon polaritons waveguides doped with lead-sulfide quantum dots as a near infra-red gain medium. A loss compensation of ~33% (an optical gain of ~143 cm<sup>-1</sup>) was observed in the guided mode. The mode propagation, coupling efficiency and stimulated emission were characterized using leakage radiation microscopy. The guided mode signature was separated using spatial filters in the Fourier plane of the microscope for quantitative measurements of stimulated emission.

©2012 Optical Society of America

**OCIS codes:** (240.6680) Surface plasmons; (250.4480) Optical amplifiers; (250.5403) Plasmonics; (230.3120) Integrated optics devices.

---

## References and links

1. H. Raether, *Surface Plasmons on Smooth and Rough Surfaces and on Gratings* (Springer, 1988).
2. W. L. Barnes, A. Dereux, and T. W. Ebbesen, "Surface plasmon subwavelength optics," *Nature* **424**(6950), 824–830 (2003).
3. V. S. Volkov, Z. Han, M. G. Nielsen, K. Leosson, H. Keshmiri, J. Gosciniak, O. Albrechtsen, and S. I. Bozhevolnyi, "Long-range dielectric-loaded surface plasmon polariton waveguides operating at telecommunication wavelengths," *Opt. Lett.* **36**(21), 4278–4280 (2011).
4. I. P. Radko, J. Fiutowski, L. Tavares, H.-G. Rubahn, and S. I. Bozhevolnyi, "Organic nanofiber-loaded surface plasmon-polariton waveguides," *Opt. Express* **19**(16), 15155–15161 (2011).
5. T. Holmgaard, Z. Chen, S. I. Bozhevolnyi, L. Markey, A. Dereux, A. V. Krasavin, and A. V. Zayats, "Wavelength selection by dielectric-loaded plasmonic components," *Appl. Phys. Lett.* **94**(5), 051111 (2009).
6. V. Coello, T. Søndergaard, and S. I. Bozhevolnyi, "Modeling of a surface plasmon polariton interferometer," *Opt. Commun.* **240**(4-6), 345–350 (2004).
7. I. P. Radko, A. B. Evlyukhin, A. Boltasseva, and S. I. Bozhevolnyi, "Refracting surface plasmon polaritons with nanoparticle arrays," *Opt. Express* **16**(6), 3924–3930 (2008).
8. V. Coello and S. I. Bozhevolnyi, "Surface plasmon polariton excitation and manipulation by nanoparticle arrays," *Opt. Commun.* **282**(14), 3032–3036 (2009).
9. T. Søndergaard and S. I. Bozhevolnyi, "Vectorial model for multiple scattering by surface nanoparticles via surface polariton-to-polariton interactions," *Phys. Rev. B* **67**(16), 165405 (2003).
10. T. Holmgaard and S. I. Bozhevolnyi, "Theoretical analysis of dielectric-loaded surface plasmon-polariton waveguides," *Phys. Rev. B* **75**(24), 245405 (2007).
11. A. Kumar, J. Gosciniak, T. B. Andersen, L. Markey, A. Dereux, and S. I. Bozhevolnyi, "Power monitoring in dielectric-loaded surface plasmon-polariton waveguides," *Opt. Express* **19**(4), 2972–2978 (2011).
12. J. Gosciniak, T. Holmgaard, and S. I. Bozhevolnyi, "Theoretical analysis of long-range dielectric-loaded surface plasmon polariton waveguides," *J. Lightwave Technol.* **29**(10), 1473–1481 (2011).
13. J. Grandidier, S. Massenet, G. des Francs, A. Bouhelier, J.-C. Weeber, L. Markey, A. Dereux, J. Renger, M. U. González, and R. Quidant, "Dielectric-loaded surface plasmon polariton waveguides: Figures of merit and mode characterization by image and Fourier plane leakage microscopy," *Phys. Rev. B* **78**(24), 245419 (2008).
14. D. J. Bergman and M. I. Stockman, "Surface plasmon amplification by stimulated emission of radiation: quantum generation of coherent surface plasmons in nanosystems," *Phys. Rev. Lett.* **90**(2), 027402 (2003).
15. J. Seidel, S. Grafström, and L. Eng, "Stimulated emission of surface plasmons at the interface between a silver film and an optically pumped dye solution," *Phys. Rev. Lett.* **94**(17), 177401 (2005).

16. M. A. Noginov, V. A. Podolskiy, G. Zhu, M. Mayy, M. Bahoura, J. A. Adegoke, B. A. Ritzo, and K. Reynolds, "Compensation of loss in propagating surface plasmon polariton by gain in adjacent dielectric medium," *Opt. Express* **16**(2), 1385–1392 (2008).
17. M. A. Noginov, G. Zhu, M. Mayy, B. A. Ritzo, N. Noginova, and V. A. Podolskiy, "Stimulated emission of surface plasmon polaritons," *Phys. Rev. Lett.* **101**(22), 226806 (2008).
18. I. De Leon and P. Berini, "Amplification of long-range surface plasmons by a dipolar gain medium," *Nat. Photonics* **4**(6), 382–387 (2010).
19. M. Ambati, S. H. Nam, E. Ulin-Avila, D. A. Genov, G. Bartal, and X. Zhang, "Observation of stimulated emission of surface plasmon polaritons," *Nano Lett.* **8**(11), 3998–4001 (2008).
20. V. I. Klimov, A. A. Mikhailovsky, S. Xu, A. Malko, J. A. Hollingsworth, C. A. Leatherdale, H.-J. Eisler, and M. G. Bawendi, "Optical gain and stimulated emission in nanocrystal quantum dots," *Science* **290**(5490), 314–317 (2000).
21. J. Grandidier, G. C. des Francs, S. Massenot, A. Bouhelier, L. Markey, J.-C. Weeber, C. Finot, and A. Dereux, "Gain-assisted propagation in a plasmonic waveguide at telecom wavelength," *Nano Lett.* **9**(8), 2935–2939 (2009).
22. P. M. Bolger, W. Dickson, A. V. Krasavin, L. Liebscher, S. G. Hickey, D. V. Skryabin, and A. V. Zayats, "Amplified spontaneous emission of surface plasmon polaritons and limitations on the increase of their propagation length," *Opt. Lett.* **35**(8), 1197–1199 (2010).
23. P. Berini and I. De Leon, "Surface plasmon-polariton amplifiers and lasers," *Nat. Photonics* **6**(1), 16–24 (2011).
24. I. P. Radko, M. G. Nielsen, O. Albrechtsen, and S. I. Bozhevolnyi, "Stimulated emission of surface plasmon polaritons by lead-sulphide quantum dots at near infra-red wavelengths," *Opt. Express* **18**(18), 18633–18641 (2010).

## 1. Introduction

Plasmonics has become an attractive research area since it has the potential to combine the fast response time of photonics and the sub-wavelength confinement of surface plasmon polaritons (SPPs) [1, 2]. Several of these studies focus on the development and characterization of passive plasmonic devices such as waveguides [3, 4], wavelength-selective filters [5], interferometers [6] and refractive elements [7], among others [8, 9]. In this context, dielectric-loaded SPP waveguides (DLSPWs) have drawn special attention in the last years due to their ability to provide subwavelength transversal confinement to SPPs. Such a confined mode is called dielectric-loaded SPP (DLSP) [10–12]. DLSPWs are strips of a dielectric material (typically poly-methyl-methacrylate - PMMA) deposited on a metallic thin-film [13]. Unfortunately, increasing the confinement factor (CF) automatically results in a diminution of the mode propagation length. In order to overcome the trade-off between sub-wavelength confinement and propagation loss, gain media have been proposed to compensate ohmic loss through optical amplification [14]. In this context, optical amplification achieved with dye molecules [15–18], erbium ions [19] and quantum dots (QDs) [20–22] have been reported [23] at visible, near infra-red and telecom wavelengths with loss compensations of ~30%. We have reported earlier an optical gain of ~200 cm<sup>-1</sup> and the corresponding propagation loss compensation of ~30% for SPP at near-infrared wavelength using lead-sulfide (PbS) QDs [24]. In this paper, we report on fabrication and characterization of straight DLSPWs doped with PbS QDs for DLSP mode amplification at near infra-red wavelengths. The optical gain was quantitatively measured by detecting the stimulated emission signal impinging directly on a photodetector. The waveguides were pumped with a Nd:YAG laser at 532 nm, whereas the DLSP mode was excited with a continuous wave Ti:Sapphire tunable laser at the wavelength of 860 nm. A loss compensation of ~33% (an optical gain of ~143 cm<sup>-1</sup>) was observed in the DLSP mode. The mode propagation, coupling efficiency and stimulated emission were characterized by leakage radiation microscopy (LRM). The stimulated emission signal, which was originated only from the guided mode inside the waveguide, was separated and measured independently by inserting spatial filters in the Fourier plane of the microscope.

## 2. Active medium for DLSPWs

The active medium was prepared by mixing the PMMA with PbS QDs (Evident Technologies). The concentration of the QDs in PMMA was chosen to be 2.8x10<sup>17</sup> cm<sup>-3</sup>. The mixture was deposited by spin coating over a 70 nm thick gold film that was previously deposited by thermal evaporation on a thin (0.17 mm) glass substrate. The thickness of the

PMMA/PbS-QDs film was set to 300 nm which assures single mode operation of the DLSPW [10]. To allow toluene to evaporate, the polymer film was baked for 2 minutes at 180 °C. The fabricated structures consist of a straight waveguide having a tapered coupler at one of its ends (Fig. 1(a)). The structures were imprinted using e-beam lithography and immersed in a MIBK/IPA(1:3) solution for resist development. It was observed that for higher concentrations of PbS QDs in the PMMA, the resulting waveguides showed defects, such as cracks and undesired roughness, which affect the DLSP mode propagation. The chosen concentration allowed the fabrication of the structures with the desired properties, i.e. correct form and size as well as enough QDs in the PMMA in order to attain stimulated emission.

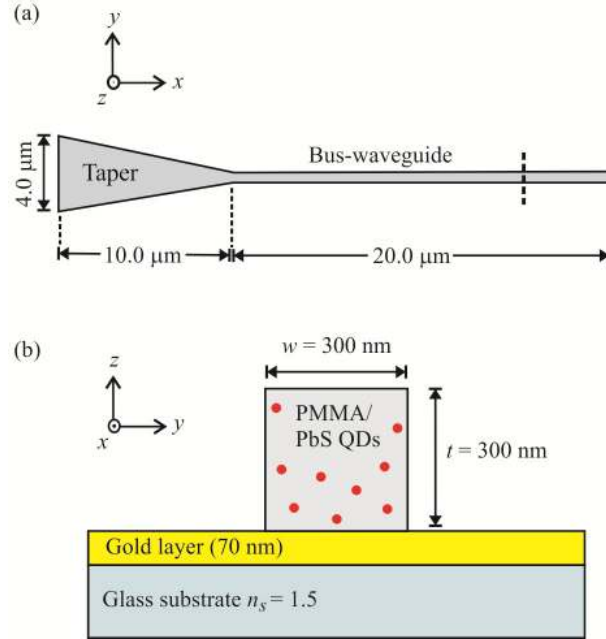


Fig. 1. (a) Straight DLSPW. (b) Cross section along the dashed line in (a). The PbS quantum dots are embedded inside the PMMA film.

### 3. Experimental setup

The experimental setup consists of a LRM arrangement composed of a 20x (NA = 0.40) focusing objective (O1) and an oil-immersion objective (O2) with high numerical aperture NA = 1.45 that was used for collecting the leakage radiation of the DLSP mode (Fig. 2(a)). A Nd:YAG laser (532 nm) was used as a pump laser and a tunable Ti:Sapphire laser set at 860 nm acted as a probe laser which coupled light into a DLSP mode inside the waveguide. The pump laser beam was expanded to cover completely the straight section of the waveguide (Fig. 2(b)). The DLSP mode is detected by collecting the corresponding leakage radiation appearing at the glass-substrate side of the sample [13]. Notice that the intensity of the leakage radiation is proportional to the intensity of the DLSP mode, making it possible to evaluate the amplification of the mode.

Both laser beams were modulated by a double-frequency chopper (2FC) at the frequencies  $f_1 = 200$  Hz and  $f_2 = 280$  Hz connected to a lock-in amplifier (LIA). The difference frequency  $\Delta f = 80$  Hz was used to detect the stimulated emission signal acquired from the structure. The incoming light from the pump laser was completely filtered out, after it has interacted with the sample (S), using band-pass filters (BPF), and neutral density filters (NDF) were used to attenuate the probe laser intensity in order to avoid saturation in the photodetector (PD).

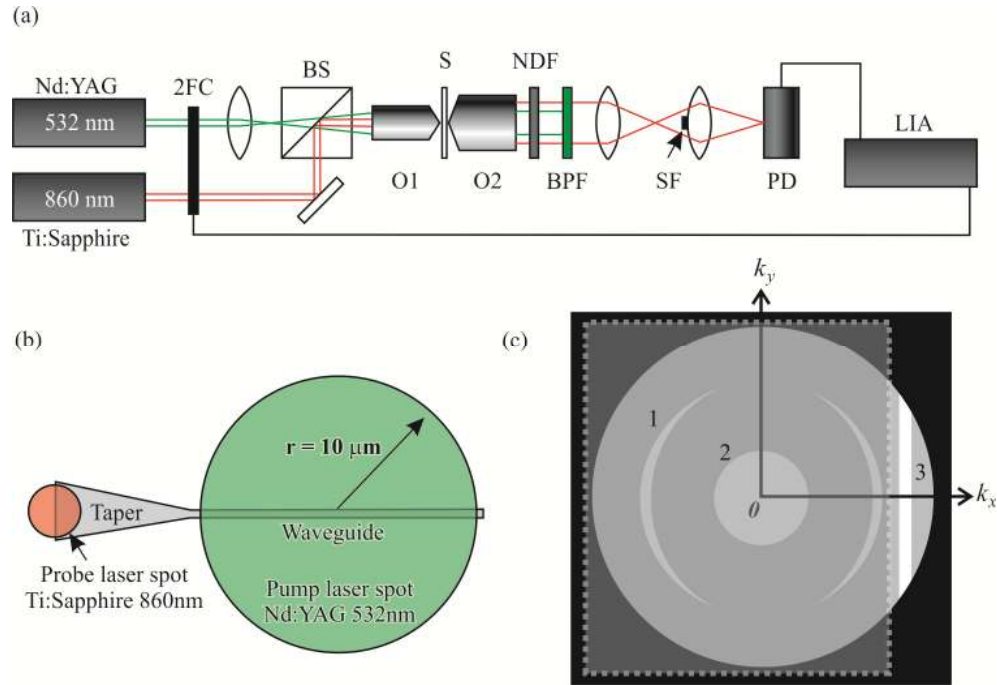


Fig. 2. (a) Experimental setup. A beam-splitter (BS) is used to combine both laser beams. (b) Active DLSPW. The small circle in the left represents the size and position where the probe laser spot was focused to couple into a DLSP mode inside the waveguide and the big circle corresponds to the pump laser. (c) Schematic of the Fourier plane showing the three main contributions: the gold-air SPP (1), the incident beam (2) and a straight line that corresponds to the guided mode signature (3). The shaded rectangle represents the spatial filter used in the experimental setup and only (3) reached the detector.

A spatial filter (SF) was placed in the Fourier plane of the microscope to eliminate all spatial frequencies which are different from the  $k$ -vector of the guided DLSP mode. The guided mode is represented by a straight line in the Fourier plane and can be easily filtered out (Fig. 2(c)). Another lens was used for focusing the transmitted through the filter light onto the photodetector. This experimental setup allowed the measurement of either spontaneous or stimulated emission inside the DLSPW by supplying the appropriate reference frequency to the LIA ( $f_1$  or  $\Delta f$ , respectively).

#### 4. Results and discussion

The propagation length of the DLSP mode was numerically calculated (using finite element method) giving a value of  $11.4 \mu\text{m}$ . This value corresponds to a DLSP mode loss of  $\sim 438 \text{ cm}^{-1}$ . The LRM image showed good confinement and effective guiding of the mode through the DLSPW (Fig. 3(a)). The oscillations of the intensity along the profile are common in LRM technique and arise from interference of the main LRM signal with close spatial components, such as those leaking from a mode in the taper region, which has different effective index (Fig. 3(b)).

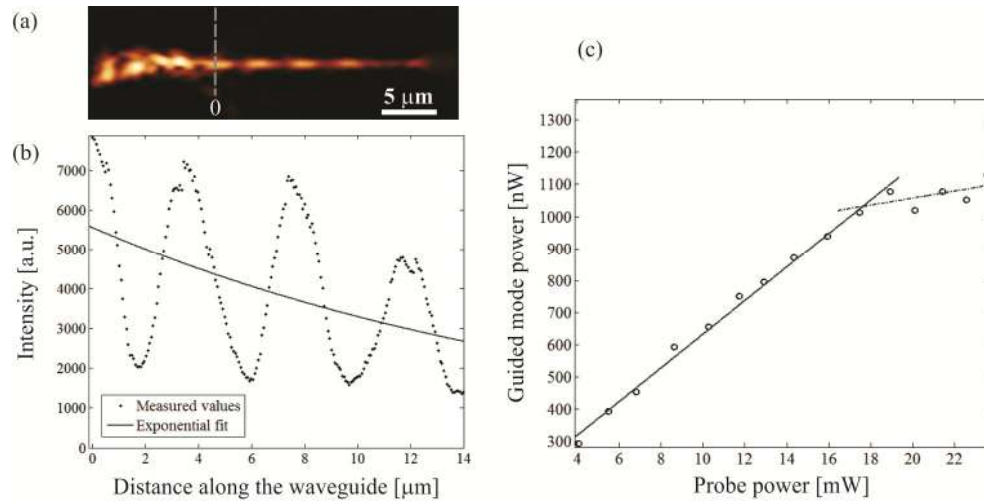


Fig. 3. (a) LRM image of the DLSPP mode propagating along the waveguide. (b) Intensity profile of the guided mode along the waveguide. (c) Guided mode power plotted for different values of the probe laser power in the absence of the pump laser.

We next measure the coupling efficiency and the stimulated emission signal. For this purpose, the probe laser beam is coupled into the DLSPPW by focusing the Gaussian beam to a spot size of  $5\mu\text{m}$  on the edge of the taper side of the waveguide, (Fig. 2(b)). Three main contributions can be observed in the Fourier plane of the microscope (Fig. 2(c)): the one from the gold/air SPP, the directly transmitted light and the corresponding contribution from the DLSPP mode. A spatial filter is placed in such a way that only the signature corresponding to the guided mode reaches the photodetector (Fig. 2(c)). The power corresponding to the DLSPP mode is measured for different values of probe power in the absence of the pump (Fig. 3(c)). This dependence must be linear and thus the coupling efficiency can be estimated directly from the slope of the curve [24]. The efficiency evaluation indicates very weak coupling into the waveguide ( $\sim 0.006\%$ ) probably due to imperfections in the structure. The dependence of the guided mode power on the probe power exhibits a change in the slope when the probe power exceeds 17 mW. The slope decreases indicating even lower coupling efficiency that can be explained by a physical damage of the PMMA film that constitutes the taper. This result indicates a reliable range of the probe power ( $\leq 16$  mW) for measurements of stimulated emission. The PMMA with embedded PbS QDs can act as an active medium if the stimulated emission couples into a DLSPP mode in the waveguide [17]. In such a case, optical amplification can be achieved resulting in an increment of the propagation length. An effective and non-destructive irradiance interval for the pump laser was found (between 1000 and  $4500\text{ W/cm}^2$ ). Stimulated emission measurements below this interval are almost in the noise level ( $\sim 50$  nW) and higher powers start to melt the PMMA film. An optical gain of  $\sim 143\text{ cm}^{-1}$  was measured for a probe power of 16 mW and pump irradiance of  $\sim 4460\text{ W/cm}^2$ , which corresponds to a compensation of  $\sim 33\%$  of the DLSPP mode loss (Fig. 4(a)). The linear dependence of stimulated emission, when measured against pump power, indicates that population inversion is completely achieved for a pump irradiance higher than  $1000\text{ W/cm}^2$  (Fig. 4(b)).

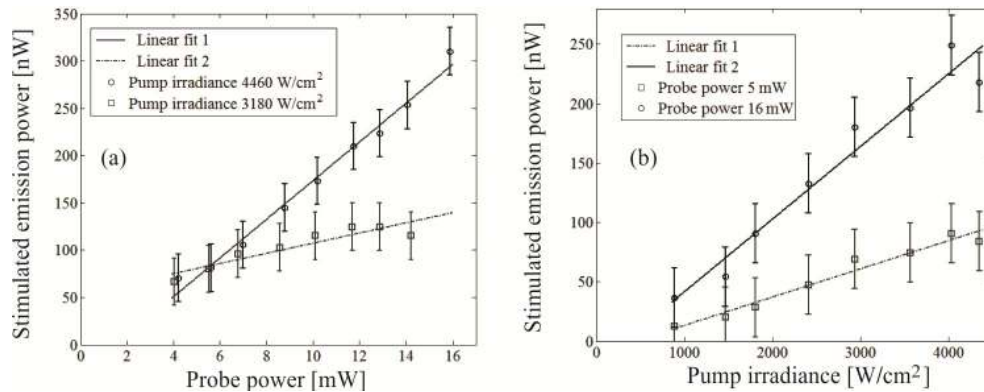


Fig. 4. (a) Stimulated emission measured for different powers of the probe laser. Two values of the pump irradiance are also shown. (b) Stimulated emission dependence measured for different values of the pump irradiance at fixed probe power. Two different values of probe laser powers are plotted.

Here, one should take into account that QDs suffer from photobleaching which is accelerated when pumping the QDs. The photoluminescence of the QDs decreased continuously during the course of the experiments, therefore, affecting the reproducibility of the experiments. When the stimulated emission power was measured for two different values of the pump irradiance (Fig. 4(a)), the first set of measurements led to slight QDs photobleaching (at pump irradiance of 3180 W/cm<sup>2</sup>) which resulted in lower initial values of the stimulated emission in the second set of measurements (at pump irradiance of 4460 W/cm<sup>2</sup>) and in an apparent intersection of the linear fit. Nevertheless, it is clear that higher values of stimulated emission were achieved for higher powers of the probe laser.

## 5. Conclusions

We have demonstrated the feasibility of separating and measuring quantitatively the stimulated emission signal that was originated only from the DLSPP mode that propagates along the waveguide. This alternative constitutes an important improvement in the detection of stimulated emission signals along DLSPPWs. The optical amplification of DLSPP guided mode was achieved at near infra-red wavelengths. An optical gain of  $\sim 143$  cm<sup>-1</sup>, which corresponds to  $\sim 33\%$  of loss compensation, was evaluated from the experiments. The inherent photobleaching and low stability of the QDs hinder reproducibility, and thus complicates the statistical treatment of experimental data. However, in this work, optical amplification and relative stability of the QDs was observed for low pump irradiances. Based on the results obtained here, as well as in previous works [15–24], we conclude that it is in general rather difficult to obtain loss compensation above  $\sim 30\%$  due to the thermal damage of the structures and active medium photobleaching. Hence, a search of new, more promising, active media for amplification of plasmonic modes remains to be an open problem.

## Acknowledgments

This work was supported by the Facultad de Ciencias Fisico-Matematicas-UANL as well as from CONACyT project SEP CONACYT I0C006-2010 and scholarship 228959. Authors also appreciate the support of the Danish Council for Independent Research (FTP-project No. 09-072949 ANAP). Z. Han would like to acknowledge the support from the National Natural Science Foundation of China (grant 61107042).